Identification of a $Ni_{0.5}(Al_{0.5-x}Mn_x)$ B2 phase at the heterophase interfaces of Cu-rich precipitates in an α-Fe matrix

R. Prakash Kolli,[a] Zugang Mao, and David N. Seidman[b]
Department of Materials Science and Engineering, Northwestern University, Evanston, Illinois 60208, USA

Denis T. Keane
DND-CAT, Northwestern University Synchrotron Research Center, Argonne, Illinois 60439, USA

(Received 22 August 2007; accepted 10 November 2007; published online 11 December 2007)

A phase with the stoichiometry $Ni_{0.5}(Al_{0.5-x}Mn_x)$ is observed at heterophase interfaces of Cu-rich precipitates in an α-Fe matrix, utilizing atom-probe tomography. First-principles calculations are utilized to determine the substitutional energies, yielding $E_{Mn\rightarrow Ni}=0.916$ eV atom^{-1} and $E_{Mn\rightarrow Al}=-0.016$ eV atom^{-1} indicating that the manganese atoms prefer substituting at Al sublattice sites instead of Ni sites. A synchrotron radiation experiment demonstrates that the identified phase possesses the B2 structure. © *2007 American Institute of Physics*. [DOI: 10.1063/1.2820378]

Precipitation strengthening of steels by nanoscale Cu-rich precipitates yields commercial steels with excellent mechanical properties.[1] The presence of solute elements such as Ni, Al, and Mn affects significantly the kinetics and thermodynamics of phase decomposition when compared to model binary Fe–Cu alloys.[2–10] These solute elements have been observed within the precipitate cores and at the Cu-rich precipitate/α-Fe matrix interfaces by experiment[2–5] and simulation.[8,9] Interfacial segregation of Ni, Al, and Mn at Cu-rich precipitate/α-Fe matrix interfaces reduces the interfacial free energy,[9–13] thereby decreasing the coarsening rate. Furthermore, the Ni, Al, and Mn concentrations[2–4,8,13] and stoichiometric ratio of Ni:Al:Mn at the heterophase interfaces[3,4,13] are observed to evolve temporally. These recent results for precipitation strengthened multicomponent steels are suggestive, based on stoichiometry alone, of a $Ni_{0.5}(Al_{0.5-x}Mn_x)$ phase (B2 structure) at these heterophase interfaces, with Mn substituting at Al sublattice sites. Equiatomic NiAl possesses the ordered cubic B2 (CsCl) structure ($cP2$, $Pm\bar{3}m$).[14] Furthermore, Cahn's local phase rule for heterophase interfaces[15] determines that a single phase is thermodynamically possible at a heterophase interface. Additionally, our recent THERMO-CALC results predict the formation of a NiAl phase at temperatures near 500 °C, indicating that a NiAl phase is thermodynamically possible for these steels.[3,4] Therefore, the likelihood of a phase found at the Cu-rich precipitate/α-Fe matrix heterophase interfaces in the steels being studied is compelling.

In this article, we present results from local electrode atom probe (LEAP™) tomography,[16] first-principles calculations, and a synchrotron radiation experiment performed at the Advanced Photon Source (APS), Argonne National Laboratory, which demonstrate that the observed interfacial segregation phase possesses the B2 structure with Mn substituting at Al sublattice sites. An Fe–0.21 C–1.82 Cu–2.67 Ni–1.38 Al–0.51 Mn–1.0 Si–0.04 Nb (at. %) steel was solutionized at 900 °C for 1 h in the γ-Fe (fcc) phase range and quenched in water at 25 °C yielding a ferritic (bcc) microstructure.[13] The steel was aged subsequently for 1024 h at 500 °C.

The LEAP tomographic specimens were cut and then electropolished into tips. The experiment was conducted at a specimen temperature of 50 K, ultrahigh vacuum of 1.1×10^{-8} Pa, a pulse fraction of 20%, and pulse repetition rate of 200 kHz, collecting $\sim3\times10^6$ ions in a $36\times37\times93$ nm^3 volume. The computer program IVAS (Imago Scientific Instruments) is used to analyze the data. The distribution of atoms for two representative precipitates [Figs. 1(a) and 1(b)] demonstrates clearly the presence of a Cu-rich core

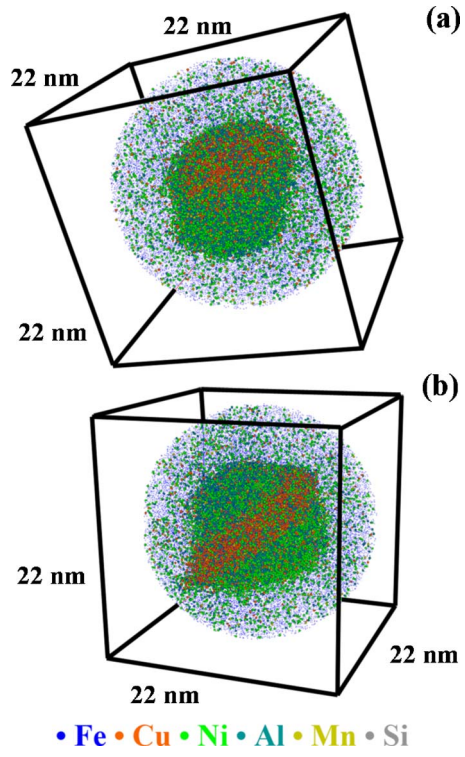

FIG. 1. (Color online) LEAP tomographic reconstructions of representative precipitates from an Fe–0.21 C–1.82 Cu–2.67 Ni–1.38 Al–0.51 Mn–1.0 Si–0.04 Nb (at. %) steel solutionized at 900 °C for 1 h and, subsequently, aged at 500 °C for 1024 h, illustrating the distribution of Fe (blue), Cu (orange), Ni (green), Al (teal), Mn (mustard), and Si (gray) atoms. Only 20% of the Fe atoms and 50% of the enlarged (not to scale) Cu, Ni, Al, and Mn atoms are displayed for clarity.

[a]Electronic mail: p-kolli@northwestern.edu.
[b]Electronic address: d-seidman@northwestern.edu

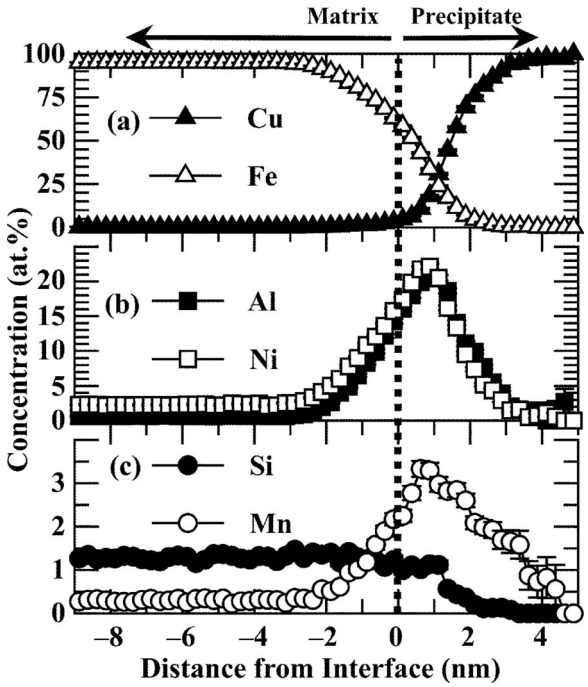

FIG. 2. Proximity histogram concentration profiles (at. %) for: (a) Cu and Fe; (b) Al and Ni; and (c) Mn and Si. The $\pm 2\sigma$ error bars are statistical uncertainties, where $\sigma=\sqrt{c_i(1-c_i)/N_{\mathrm{tot}}}$ for atomic fraction c_i and N_{tot} total atoms.

with interfacial segregation of Ni, Al, and Mn. The spheroidal shape [Fig. 1(a)] of Cu atoms is a characteristic of a 9R structure, whereas the rodlike shape [Fig. 1(b)] is indicative of a fcc structure.[6] A proximity histogram[17] concentration profile quantifies the segregation of Ni, Al, and Mn [Figs. 2(a)–2(c)]. The peak concentrations of Ni (22.1±0.8 at. %) and Al (21.2±0.8 at. %) are collocated at a distance of 0.875 nm, whereas that of Mn (3.3±0.3 at. %) is broader and found between 0.625 and 0.875 nm. An integral sum of the ions determines the stoichiometric ratio of Ni:Al:Mn at the heterophase interfaces, yielding 0.51:0.41:0.08, which is suggestive of a $Ni_{0.5}(Al_{0.5-x}Mn_x)$, where $x=0.08$, phase with Mn substituting at Al sublattice sites. The LEAP tomographic results are indicative of a heterogeneous nucleation process. The complex kinetics demonstrate initial precipitation of the Cu-rich cores with interfacial segregation of Ni, Al and Mn.[3,4,13] Further aging results in increased segregation of Ni, Al, and Mn to the heterophase interfaces and temporal evolution of the Ni:Al:Mn stoichiometric ratio,[3,4,13] resulting in the observed phase.

To determine the sublattice preference of Mn, first-principle calculations are performed using the plane wave pseudopotential total energy method with local density approximation,[18] as implemented in the Vienna *ab initio* simulation package (VASP).[19,20] The electron-ion interaction used is the ultrasoft pseudopotential[21] with plane waves up to an energy cutoff of 300 eV, $4\times4\times4$ Monkhorst-Pack *k*-point grids. A three-dimensional periodic supercell with $2\times2\times2$ unit cells is employed to determine the total energies of the calculated cells. The energy per unit cell converged to 2×10^{-5} eV atom^{-1} and the residual forces to 0.005 eV nm^{-1}. The lattice parameters and atoms of an equiatomic NiAl B2 crystal are fully relaxed. The lattice parameter is determined to be 0.2834 nm, which is in excellent agreement with the experimental value of 0.28770±0.00001 nm.[14] The two substitutional structures, $(Ni_{0.5-y}Mn_y)Al_{0.5}$ and $Ni_{0.5}(Al_{0.5-x}Mn_x)$, are fully relaxed. The total energies E^{tot} and substitutional energies $E_{\mathrm{Mn}\rightarrow\mathrm{Z,Z=Ni\ or\ Al}}$, which are defined as

TABLE I. Total and substitutional energies determined by first-principles calculations.

	E^{tot} (eV)	$E_{\mathrm{Mn}\rightarrow\mathrm{Z,\ Z=Ni,Al}}$ (eV atom^{-1})
NiAl	−97.5894	···
$(Ni_{0.5-y}Mn_y)Al_{0.5}$	−100.229	0.915
$Ni_{0.5}(Al_{0.5-x}Mn_x)$	−101.196	−0.016

$$E_{\mathrm{Mn}\rightarrow\mathrm{Ni}}=[(E^{\mathrm{tot}}_{(\mathrm{Ni}_{0.5-y}\mathrm{Mn}_y)\mathrm{Al}_{0.5}}+n_{\mathrm{Ni}}\mu_{\mathrm{Ni}})-(E^{\mathrm{tot}}_{\mathrm{NiAl}}+n_{\mathrm{Mn}}\mu_{\mathrm{Mn}})]/n_{\mathrm{Mn}}, \quad (1)$$

$$E_{\mathrm{Mn}\rightarrow\mathrm{Al}}=[(E^{\mathrm{tot}}_{\mathrm{Ni}_{0.5}(\mathrm{Al}_{0.5-x}\mathrm{Mn}_x)}+n_{\mathrm{Al}}\mu_{\mathrm{Al}})-(E^{\mathrm{tot}}_{\mathrm{NiAl}}+n_{\mathrm{Mn}}\mu_{\mathrm{Mn}})]/n_{\mathrm{Mn}}, \quad (2)$$

where n is the number of atoms and μ is chemical potential, are calculated and summarized in Table I. These first-principles results demonstrate that Mn atoms prefer substituting for Al instead of Ni sublattice sites.

Additionally, the strains resulting from Mn substitution at Ni sublattice sites yield an average atomic force of 0.0004 eV Å^{-1}, whereas substitution at Al sublattice sites yields 0.0002 eV Å^{-1}. No atomic force is observed after the first nearest-neighbor distance.

To determine the crystal structure of this heterophase interface phase, a powder diffraction experiment was conducted at beamline 5-ID-B, operated by DND-CAT at the APS. We calculate, assuming a spherical shell, that ~0.2% of the atoms reside at the heterophase interfaces, requiring the use of a high x-ray flux at the APS. The specimen, $0.3\times12.5\times25$ mm^3, was mounted on a standard flat-plate sample holder. The beamline energy was nominally 17 462 eV with a wavelength $\lambda=0.71$ Å. The sample was measured in a symmetric Bragg condition with the sample rocking through 3° per step, during a theta (θ)/two-theta (2θ) scan of 0.0075° 2θ steps, 100 s/point. The high-resolution multidetector powder camera utilizes 11 Si(111) crystal analyzers situated at ~2° intervals in 2θ with Oxford Cyberstar scintillation counters for each analyzer; only detectors 1 and 2 are used for the data shown in Fig. 3.

Calculations of relative intensities indicate that the three strongest 2θ reflections for $Ni_{0.51}(Al_{0.41}Mn_{0.08})$ (B2 structure) are within 0.18° of the three strongest bcc Fe reflections. Furthermore, the superlattice reflections are relatively weak, which are reduced further in intensity since the scattering factors obey the condition $f_{\mathrm{Mn}}>f_{\mathrm{Al}}$. The calculated 2θ reflection at 14.18° (100), however, is not convoluted with a reflection from another phase. The powder diffraction results (Fig. 3) demonstrate clearly a 2θ reflection at ~14.14°, $d\cong0.2884$ nm.

The observed reflection may possibly be the result of homogeneously distributed $Ni_{0.5}(Al_{0.5-x}Mn_x)$ precipitates. We have detected, however, only one such precipitate in all LEAP tomographic data sets acquired. Furthermore, the single observed precipitate was at 64 h aging rather than 1024 h. The absence of homogeneously distributed precipi-

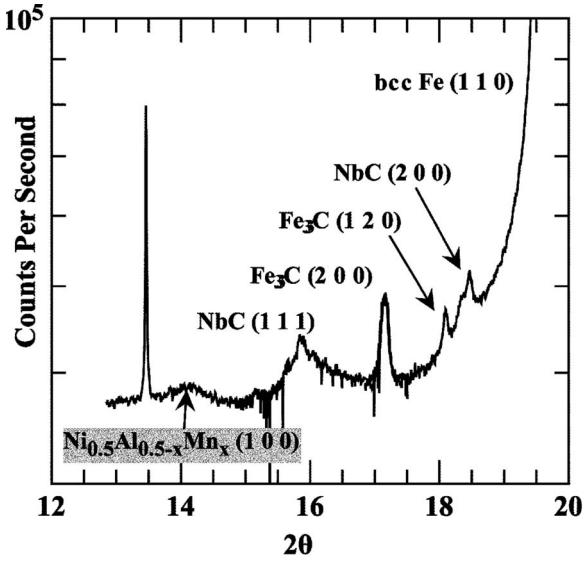

FIG. 3. Powder diffraction results for an Fe–0.21 C–1.82 Cu–2.67 Ni–1.38 Al–0.51 Mn–1.0 Si–0.04 Nb (at. %) steel solutionized at 900 °C for 1 h, and, subsequently aged at 500 °C for 1024 h. The peak at 13.4° could not be identified.

tates and the observation of a $Ni_{0.5}(Al_{0.5-x}Mn_x)$ phase at the heterophase interfaces and the previously reported existence of similar precipitates at a grain boundary[1] indicate that the driving force for homogeneous nucleation within the α-Fe matrix is most likely insufficient for the given alloy composition and thermal treatments. Therefore, we conclude that homogeneously distributed $Ni_{0.5}(Al_{0.5-x}Mn_x)$ precipitates do *not* contribute significantly to the observed reflection.

This research is supported by the Office of Naval Research under Contract No. N00014-03-1-0252. Atom-probe tomographic analyses were performed at the Northwestern University Center for Atom-Probe Tomography (NUCAPT). The LEAP™ tomograph was purchased with funding from the National Science Foundation and the Office of Naval Research. Portions of this work were performed at the DuPont-Northwestern-Dow Collaborative Access Team (DND-CAT) located at Sector 5 of the Advanced Photon Source (APS). DND-CAT is supported by E.I. DuPont de Nemours & Co., The Dow Chemical Company, and the State of Illinois. Use of the APS was supported by the US Department of Energy, Office of Science, Office of Basic Energy Sciences under Contract No. DE-AC02-06CH11357. We extend our gratitude to M. E. Fine, D. Isheim, and S. Vaynman for discussions.

[1] S. Vaynman, D. Isheim, R. P. Kolli, S. P. Bhat, D. N. Seidman, and M. E. Fine, High-Strength Low-Carbon (HSLC) Ferritic Steel Containing Cu-Fe-Ni-Al-Mn Precipitates, Metall. Mater. Trans. A (to be published).
[2] D. Isheim, R. P. Kolli, M. E. Fine, and D. N. Seidman, Scr. Mater. **55**, 35 (2006).
[3] R. P. Kolli and D. N. Seidman, The temporal evolution of the decomposition of a concentrated multicomponent Fe-Cu based steel (unpublished).
[4] R. P. Kolli, R. M. Wojes, S. Zaucha, and D. N. Seidman, A subnanoscale study of the nucleation, growth, and coarsening kinetics of Cu-rich precipitates in a multicomponent Fe-Cu based steel (unpublished).
[5] G. M. Worrall, J. T. Buswell, C. A. English, M. G. Hetherington, and G. D. W. Smith, J. Nucl. Mater. **148**, 107 (1987).
[6] P. J. Othen, M. L. Jenkins, and G. D. W. Smith, Philos. Mag. A **70**, 1 (1994).
[7] K. Osamura, H. Okuda, K. Asano, M. Furusaka, K. Kishida, F. Kurosawa, and R. Uemori, ISIJ Int. **34**, 346 (1994).
[8] T. Koyama, K. Hashimoto, and H. Onodera, Mater. Trans. **47**, 2765 (2006).
[9] C. Zhang and M. Enomoto, Acta Mater. **54**, 4183 (2006).
[10] A. Seko, S. R. Nishitani, I. Tanaka, H. Adachi, and E. F. Fujita, CALPHAD: Comput. Coupling Phase Diagrams Thermochem. **28**, 173 (2004).
[11] R. P. Kolli, K. E. Yoon, and D. N. Seidman, Comparisons of interfacial excess formalisms for segregation at precipitate/matrix heterophase interfaces (unpublished).
[12] D. Isheim, M. S. Gagliano, M. E. Fine, and D. N. Seidman, Acta Mater. **54**, 841 (2006).
[13] R. P. Kolli, "Kinetics of nanoscale Cu-rich precipitates in a multicomponent concentrated steel," Ph.D. thesis, Northwestern University, 2007.
[14] D. B. Miracle, Acta Metall. Mater. **41**, 649 (1993).
[15] J. W. Cahn, J. Phys. (Paris), Colloq. **43**, 199 (1982).
[16] T. F. Kelly and D. J. Larson, Mater. Charact. **44**, 59 (2000).
[17] O. C. Hellman, J. A. Vandenbroucke, J. Rüsing, D. Isheim, and D. N. Seidman, Microsc. Microanal. **6**, 437 (2000).
[18] G. Kresse and J. Hafner, Phys. Rev. B **47**, 558 (1993).
[19] R. O. Jones and O. Gunnarsson, Rev. Mod. Phys. **61**, 689 (1989).
[20] A. Lindbaum, J. Hafner, E. Gratz, and S. Heathman, J. Phys.: Condens. Matter **10**, 2933 (1998).
[21] A. Lindbaum, J. Hafner, and E. Gratz, J. Phys.: Condens. Matter **11**, 1177 (1999).